Eur Food Res Technol (2012) 235:1083–1091
DOI 10.1007/s00217-012-1837-1

ORIGINAL PAPER

Impact of flavour solvent on biscuit micro-structure as measured by X-ray micro-Computed Tomography and the distribution of vanillin and HMF (HPLC)

Ni Yang · Ian D. Fisk · Robert Linforth · Keith Brown · Stuart Walsh · Sacha Mooney · Craig Sturrock · Joanne Hort

Received: 6 July 2012 / Revised: 7 September 2012 / Accepted: 15 September 2012 / Published online: 4 October 2012

Abstract The influence of flavour solvent, propylene glycol (PG) and triacetin (TA), was investigated on the micro-structure (as measured by X-ray micro-Computed Tomography, X-ray μCT) and aroma compound distribution (as measured by HPLC) within shortcake biscuits. X-ray μCT scanning showed biscuits made with PG had smaller pores and higher porosity than biscuits made with TA. Vanillin distribution across the biscuits was not homogeneous and was found at higher concentrations in the centre of the biscuits than the edge or bottom. The baked aroma compound 5-hydroxymethyl-furfural (HMF) was present at higher concentrations at the surface of the biscuits where Maillard chemistry is presumed to occur at its highest rate. The type of solvent had a significant effect on the total concentration and distribution of aroma compounds ($p < 0.05$). TA biscuits retained greater vanillin and more HMF was formed during baking when compared to PG biscuits. The core of TA biscuits had (on a relative scale) a much greater vanillin and lower HMF concentration than PG biscuits when compared to their periphery. Although this may be due to different physicochemical properties of the two solvents and varying levels of interactions with other ingredients, the micro-structure differences indicated by X-ray μCT image analysis illustrate one potential route by which the flavour solvent may be influencing the generation and stability of biscuit aroma compounds.

Keywords Food structure · Snack foods · Aroma · Biscuit · X-ray μCT

N. Yang · I. D. Fisk (✉) · R. Linforth · J. Hort
Division of Food Sciences, University of Nottingham, Sutton Bonington Campus, Sutton Bonington, Loughborough, Leicestershire LE12 5RD, UK
e-mail: Ian.Fisk@nottingham.ac.uk

K. Brown · S. Walsh
Aromco Ltd, Bell Farm Industrial Park Nuthampstead, Hertfordshire SG8 8ND, UK

S. Mooney · C. Sturrock
Division of Agricultural and Environmental Sciences, University of Nottingham, Sutton Bonington Campus, Loughborough, Leicestershire LE12 5RD, UK

Introduction

Flavourings are commonly divided into classes based on their physical states, for example, liquid, emulsions, powder or paste. Typically liquid flavourings are made by blending the required flavouring substances, in the desired concentration, with particular food-grade solvents. Selecting an appropriate solvent for a liquid flavouring is normally based on its ability to dissolve the required flavouring compounds and its solubility in the food products to which it is to be applied. Two commonly used solvents in the global flavouring industry are propylene glycol (PG) and triacetin (TA), which are the main solvents of interest in this study.

Propylene glycol (1,2-propanediol) is a colourless, slightly viscous liquid with a faintly sweet taste [1]. Since it is miscible with water, alcohol and many flavour compounds, and relatively inexpensive, it is an extensively used flavour solvent in the food industry. The chemical structure of propylene glycol is well known and contains two hydroxyl groups that can directly react with some flavour compounds including vanillin. The flavour carrier solvent can also interact with the food matrix in a number of ways either through chemical reactions or physical modifications [2].

PG can react specifically with aldehydes and ketones to form acetals and ketals [3]. For instance, cinnamaldehyde and vanillin could form cinnamaldehyde propylene glycol acetal and vanillin propylene glycol acetal [4, 5]. In addition to PG-acetal formation, Elmore [5] summarised two other reaction pathways that can occur during the storage of PG flavourings: reactions between PG and organic acids commonly used in flavourings (e.g. acetic and butyric acid) to form both monoesters and diesters; and the transesterification of lactones to give dihydroxy esters in stored flavourings.

Compared to PG, triacetin (1,2,3-propanetriol triacetate) is a colourless, slightly viscous liquid with a very faint ethereal-fruit odour [1]. TA is less polar than PG and more oil soluble. Since TA does not react with aldehydes, it can be used in flavourings where the use of PG is restricted or avoiding acetal formation becomes vital. TA has also been shown to enhance flavour stability, and Choi [6] successfully incorporated TA into oil-in-water emulsions to alter the stability of citral to chemical degradation. Their results indicated that TA improves the chemical stability of citral in a beverage emulsion.

Choice of the flavour solvent may also impact the physical properties of the food. Dr Roos [7] suggested that PG can act as a plasticiser in glassy state systems, and for hard candies, it can make the product sticky. Triacetin is widely used in the chewing gum flavouring as the gum formulated with triacetin is often softer than when formulated with propylene glycol [8]. Although there is a variety of unconnected research in different food types, it is clear that solvent choice does have the potential to impact not only product flavour but also structure. In this work, the impact of biscuit structure on flavour stability will be studied.

Food structure can be examined from a three-dimensional prospective using X-ray micro-Computed Tomography (X-ray μCT). This is a non-destructive technique for visualising solid interiors, where the X-ray attenuation of the solid food is a function of density of the material [9]. The technique involves the acquisition of a series of 2D radiograph images over a 360° rotation of the sample [10]. These radiographs are then reconstructed using filtered back projection algorithms [11] resulting in the creation of a volumetric dataset of the sample's X-ray attenuation. Image processing software permits the visualisation and quantification of the internal structure of the sample. X-ray μCT scanning has previously been applied on different types of biscuits and breadsticks [12]. Due to the novel nature of the technique and recent advances in image processing power, the impact of solvent on biscuit microstructure by X-ray μCT analysis and aroma stability has never previously been reported in the literature.

In this study, it is proposed that the combined knowledge of the spatial microstructure of shortcake biscuits and their aroma chemistry may explain the impact of solvent on the concentration of added vanillin and the generation of 5-hydroxymethyl-furfural (HMF).

Materials and methods

Materials

Food-grade vanillin, propylene glycol (PG) and triacetin (TA) were supplied by Aromco Ltd. (Nuthampstead, UK). Two simple vanilla flavours were made by mixing vanillin (10 % w/w) with PG or TA as the flavour solvent. Both flavourings were made on the day of application, the standard application dosage for both flavourings was 0.2 % w/w in the biscuit dough (i.e. 200 ppm of vanillin was added initially).

Acetovanillone (≥98 %, SAFC Supply Solutions, St. Louis, USA) was used as the internal standard (IS) for HPLC detection. Methanol (HPLC Grade ≥99.9 %) was ordered from Fisher Scientific UK Ltd, Loughborough, UK. Acetic acid (≥99.85 %) and 5-hydroxymethyl-furfural (HMF, ≥99 %) were purchased from Sigma Aldrich, UK.

Preparation of standard biscuits

Standard dough was prepared from the ingredients listed below: (1) shortening 15 g/100 g; (2) icing sugar, 15 g/100 g; (3) invert sugar, 2 g/100 g; (4) skimmed milk powder, 0.3 g/100 g; (5) salt, 0.3 g/100 g; (6) lecithin, 0.3 g/100 g; (7) sodium bicarbonate, 0.14 g/100 g; (8) ammonium bicarbonate 0.03 g/100 g; (9) water 11 g/100 g; (10) biscuit flour 56 g/100 g; (11) flavouring, 0.02 g/100 g. Shortening was supplied by Cardowan Creameries Ltd (Glasgow, UK), and the biscuit flour was sourced from Rank Hovis (High Wycombe, UK). All other ingredients were supplied by C Holland & Sons Ltd. (Royston, UK).

The ingredients from No. 1 to No. 6 were weighed and blended by a spade blender (Hobart, Windsor, UK). A fat base was then formed after 2 min of continuous mixing of these ingredients. A water base was prepared by dissolving the Ingredients No. 7 and No. 8 in cold tap water. Standard dough was made by gradually mixing flour into the fat base then added the water base into the fat base using a spade blender. The flavouring (PG or TA) was then added and blended to homogeneity by spade blender. Each dough preparation was then rolled to 40 mm thickness using a Pastry Brake (Seewer Rondon, Burgdorf, Switzerland) and shaped by a model cutter (36 mm diameter, round with fluted edge) to produce individual biscuits.

The biscuits with PG and TA flavouring were positioned in alternating rows, with equal separating distances on the

same tray to reduce baking variation. The tray of biscuits was placed on the top layer of a Deck Oven (Sveba-dahlen, Fristad, Sweden) and baked at 230 °C for 8 min on the top layer and were then dried on the bottom layer of the oven for 3 min at 100 °C. Finally, the baking tray was removed from the oven to allow the biscuits to cool for 10 min at room temperature (25 °C). Biscuits at the edge of the tray were discarded to minimise baking variation that was known to occur in these positions [13]. The biscuits were then carefully packed and stored in sealed aluminium bags with a minimum headspace within the bag, moisture content was analysed as per Fisk [14].

X-ray μCT analysis

The microstructure of three PG biscuits and three TA biscuits was analysed by X-ray μCT using a Pheonix Nanotom NF180 X-ray CT System (GE Sensing & Inspection Technologies GmbH, Wunstorf, Germany). Triplicate biscuits were fixed together in the position shown in Fig. 1a, in order to be rotated and scanned as one stack. The scan consisted of 1,440 projection images collected over a 360° rotation using an electron acceleration energy of 80 kV, a current of 180 μA and a scan resolution of 22.5 μm. A 3D rendered model of the biscuit after reconstruction is illustrated in Fig. 1b.

Image analysis

All images were analysed by 'Image J' processing software version 1.44 (public domain Java analysis programme, developed by National Institute of Health, Maryland, US) [15].

Without any physical destruction, a cross-sectioned view of the top (XY slice) and the front slice (ZX slice) for both PG and TA biscuit were extracted from the CT scan, illustrated in Fig. 2. The white areas (high X-ray attenuation) show the biscuit matrix, and the black areas (low X-ray attenuation) inside the biscuits indicate pores (air space).

A 'remove dark outliers' filter with a radius of 0.5 pixels was applied to reduce binary noise in the images. Image J was then used to analyse the average size of all the pores in a defined region of the biscuit and area fraction (also known as the porosity) using the 'Analyze Particles' function in Image J.

Hundred reprehensive XY slice images were selected per biscuit. The central region (area = 25 × 25 mm) was used in every biscuit layer and the exterior was discarded. The image analysis settings as described were applied for all six biscuit samples. A total of 300 images were generated for either PG or TA biscuits based on triplicate samples.

Additional investigations were carried out at four different blocks within one biscuit (13.5 × 9 mm) as demonstrated in Fig. 3. Similar image analysis was carried out for each block per biscuit with 100 XY image slices, therefore generating 1,200 slices in total.

Aroma distribution analysis

Replicates of standard biscuits were cut across with a sharp knife from left to right into seven pieces (A1–A7, as shown in Fig. 4). Three PG biscuits and three TA biscuits were used to assess the average vanillin and HMF concentration in each section. A further three reps of TA biscuits and PG biscuits were sectioned into four layers from top to bottom (L1–L4, as shown in Fig. 4). Similarly, each layer was weighed and vanillin and HMF concentration quantified in each layer.

Each biscuit piece (~0.11 g) was weighed and extracted with 1 ml methanol, 10 μl of the internal standard (IS) was added prior to extraction. The IS consisted of acetovanillone (100 mg) in 100 ml methanol. All samples were then placed on a roller mixer (Thermo Scientific, Tube roller Spiramix

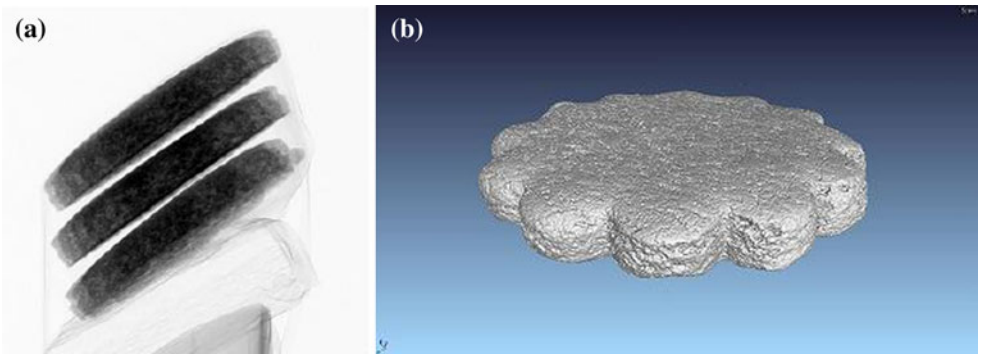

Fig. 1 **a** A X-ray radiograph image showing the arrangement of three biscuits to be scanned together; **b** 3D image of one biscuit after reconstruction

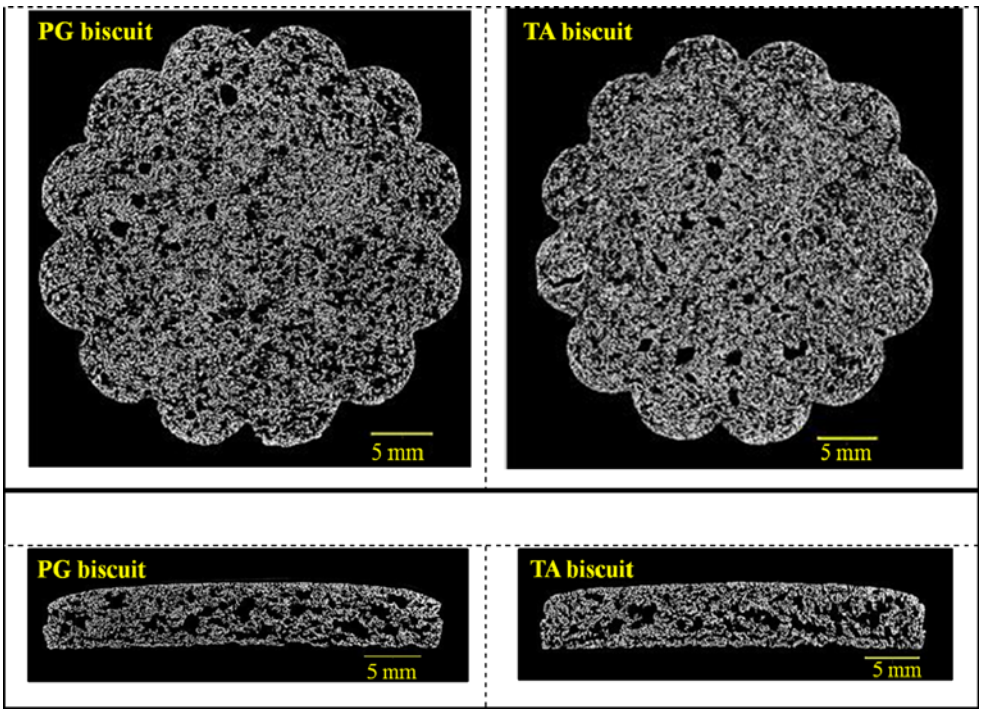

Fig. 2 Image from a *top slice* (XY) and a *front slice* (ZX) of PG and TA biscuit with 5-mm scale indicator

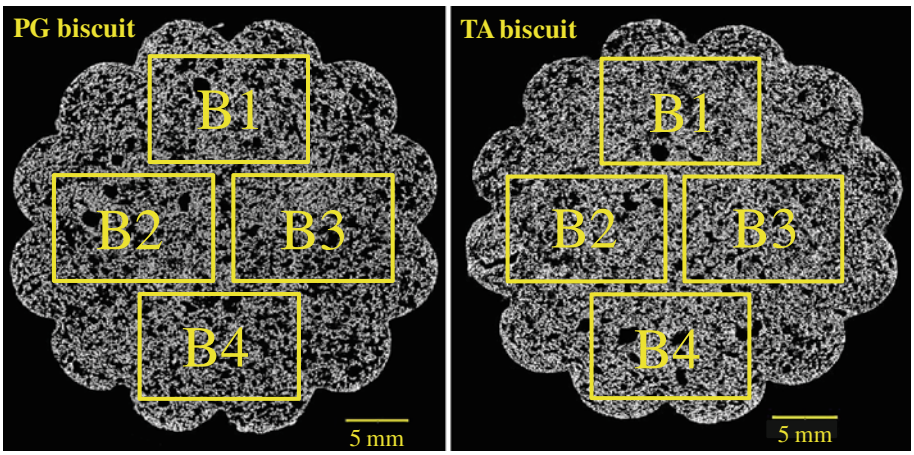

Fig. 3 Demonstration images of four blocks (*B1–B4*) selected for both PG and TA biscuit

10) to roll side by side for 30 min and then centrifuged at 1,300×*g* for 20 min at 5 °C (Thermo CR3i Multifunction Centrifuge, KeyWrite-DTM). The upper solvent layer was isolated, and 0.5 ml of the extract was filtered (nylon syringe filter 4 mm 0.4 µm) into 2-ml amber vials, capped with Teflon-coated lids and analysed by HPLC.

The HPLC (Alliance® Waters 2095, Waters Corporation, Massachusetts, USA) fitted with a photodiode array detector (PDA, Waters 996) was used. Compounds were measured at an absorption wavelength of 270 nm and separated by a C18 column (C18 Techsphere, 5 µm, 250 × 4.6 mm, Thermo Scientific, Manchester, UK). The instrumental settings were as follows: injection volume 10 µl; flow rate 1 ml per min; gradient elution with (1) water (1 % acetic acid) and (2) methanol (ramped from 20 % B v/v to 50 % B v/v over 30 min then to 100 % B v/v over 1 min and held for 2 min). The chromatography data were analysed by Millennium[32] software (Waters, USA). The retention time for authentic standard of HMF, vanillin and acetovanillone was 5.1, 15.0 and 17.9 min, respectively. Concentration (ppm, µg/g) was calculated from the ratio of the peak area of compound of interest to the peak area of internal standard.

Data analysis

All results were analysed by SPSS 16.0 (SPSS Inc., Chicago, USA) to calculate the average (AV) and standard

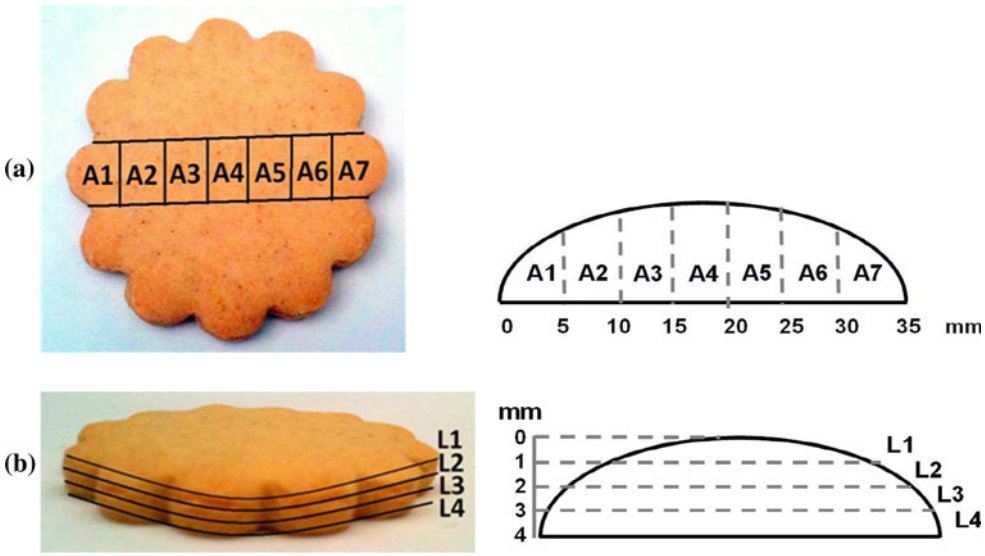

Fig. 4 Illustration of cutting a biscuit **a** across seven pieces from left to right (*A1–A7*); **b** into four layers from top to bottom (*L1–L4*)

deviation (STD) of pore size and porosity for both PG and TA biscuits. ANOVA followed by Tukey's multiple comparison tests was applied where appropriate ($p < 0.05$). Pearson's correlations with two-tailed test were applied to the distribution of vanillin and pores (porosity and average pore size) in the defined areas for both PG and TA biscuit, $p < 0.05$.

Results and discussion

Biscuits micro-structure (X-ray μCT)

The structure and moisture content of both PG and TA biscuit was analysed by X-ray μCT and showed no major differences between the solvent types after baking. Internally the biscuit contains a number of pores, the distribution of pores differed between the biscuits prepared with PG and those prepared with TA. The average pore diameter identified in PG biscuits (diameter 0.105 ± 0.008 mm) was significantly smaller ($p < 0.001$) when compared to TA biscuits (diameter 0.110 ± 0.015 mm). The average porosity (%) of PG biscuits (49.5 ± 2.4 %) was significantly greater than TA biscuits (45.4 ± 2.1 %, $p < 0.001$).

These initial results indicated that PG biscuits contained significantly more pores of smaller diameter when compared to TA biscuits. To further understand this difference, 4 regions of the biscuit, which were chosen to represent individual bites (Fig. 3), were evaluated by the same approach to calculate pore diameter. The average pore size at each block for TA biscuits was significantly larger than that of the PG biscuits (Fig. 5a) ($p < 0.05$). When ANOVA-Tukey's post hoc test was applied, a significant effect of solvent type was shown ($p < 0.001$). Similarly, the average porosity at each block was calculated for both solvent types (Fig. 5b). PG biscuits had a significantly higher porosity than TA biscuits ($p < 0.001$). Although it should be noted that due to natural product variation, significant differences were observed between some of the blocks within one solvent for both pore diameter and porosity.

The different micro-structure observed for both PG and TA biscuits may be due to the different physicochemical properties of these two solvents and their interactions during the dough production and baking process. The formation of the cellular solid (biscuit) from short dough during baking is induced by the expansion of the dough as it is subjected to pressures from the vaporisation of water and gases from leavening powders [16]. Although only a small amount of flavour solvent was added, differences in structure were observed, the differences in volatility and hydrophobicity of flavour solvent may interact with dough ingredients in different ways leading to differences in structure: PG as the more volatile and hydrophilic solvent may enhance the distribution of the aqueous phase within the dough leading to the formation of larger numbers of small pores being formed as the leavening agent releases gas from the biscuit matrix. In biscuits, fats were reported to have a delaying effect on the release of carbon dioxide during baking [17]: TA is a more heat-stable solvent with more hydrophobic properties which may have led to the formation of larger pores due to the more inhomogeneous distribution of leaving agent and delayed release during baking.

This could further be compared to work by Lara [18] who discussed the impact of the temperature of baking on biscuit volume. Biscuits baked at high temperature (i.e. rapidly heated and moisture rapidly lost) had a higher formation of internal pores, a phenomena attributed to the rapid loss of moisture and rapid gas formation, which can be compared to the addition of solvent of different

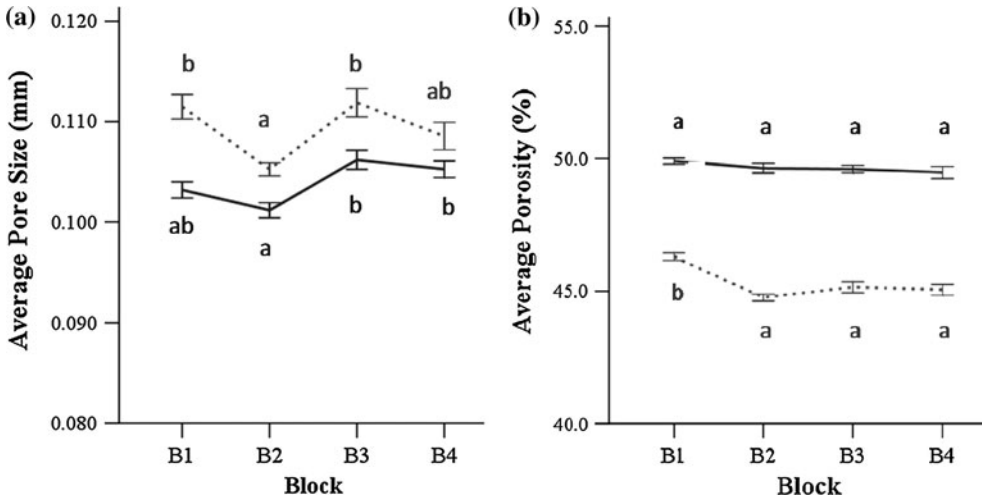

Fig. 5 Results of **a** average pore size (mm) and **b** calculated for 4 blocks (*B1–B4*) within PG biscuits (*full line*) and TA biscuits (*dotted line*). Data points are displayed with ±SE, *different letters* indicated significant different at $p < 0.05$

volatilities, the solvent with the lower volatility forming larger pores with the more volatile one forming numerous smaller pores. It should be noted that the boiling point of TA (260 °C) is not exceeded by the maximum baking temperature (max 230 °C) whilst the boiling point of PG is 188 °C.

Horizontal distribution of vanillin across the biscuit structure

The concentration of vanillin was elevated in the centre of the biscuit when compared to the horizontal extremes; this pattern was replicated in both PG and TA biscuits with similar patterns in each. Due to the small size of sample fractions, higher sample variability was observed. Therefore, to fully explain the underlying trends, all the data from each independent biscuit sample are shown for both PG (Fig. 6a) and TA biscuits (Fig. 6b). It is proposed that the extremities will be subjected to higher temperature–time profiles [19] and subsequently more rapid moisture loss [19], greater heat damage and great volatile loss [20] than the internal core samples, which accounts for the distribution profile.

Although the distribution of vanillin is comparable (Fig. 6) between PG and TA, there are subtle differences in the underlying trends. In the PG biscuit, the central 15 cm has elevated vanillin levels when compared to the extreme 5 cm, whereas in the TA biscuit, the central 20 cm retained much elevated levels when compared to the extreme 5–10 cm, this indicates that there is a central core of the TA biscuit that retains statistically elevated concentrations of vanillin. When comparing the biscuit core concentration, 160 ppm can be found in the TA biscuit, whereas the maximal concentration in the PG biscuits was only 136 ppm, this 18 % enhancement in core vanillin concentration may be of interest commercially. It should be noted that in all cases, the mean vanillin concentration in the TA biscuit exceeded that of the PG biscuit which supports our previous studies in this area [21].

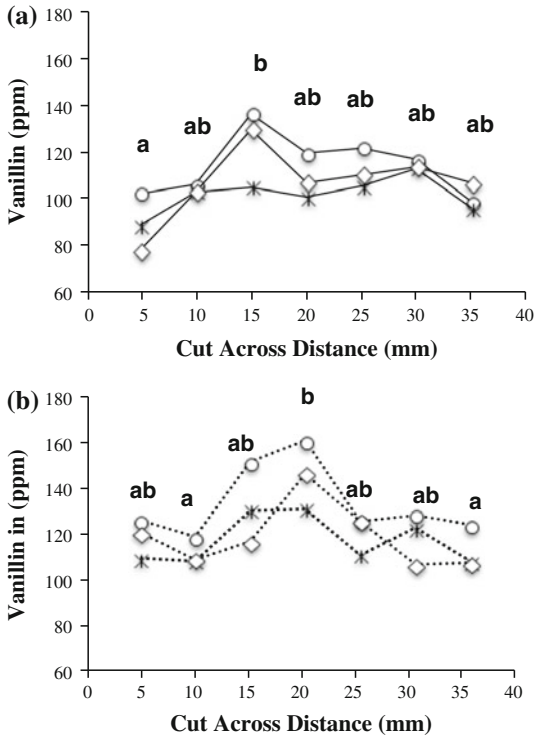

Fig. 6 Distribution of vanillin concentration (ppm) cutting across seven pieces for **a** three PG biscuits (*full lines*) and **b** three TA biscuits (*dotted lines*). *Different letters* indicated significant different levels between pieces ($p < 0.05$)

Vertical distribution of vanillin across the biscuit structure

For both PG and TA biscuits (Fig. 7), the central region contained the greatest vanillin and the upper section

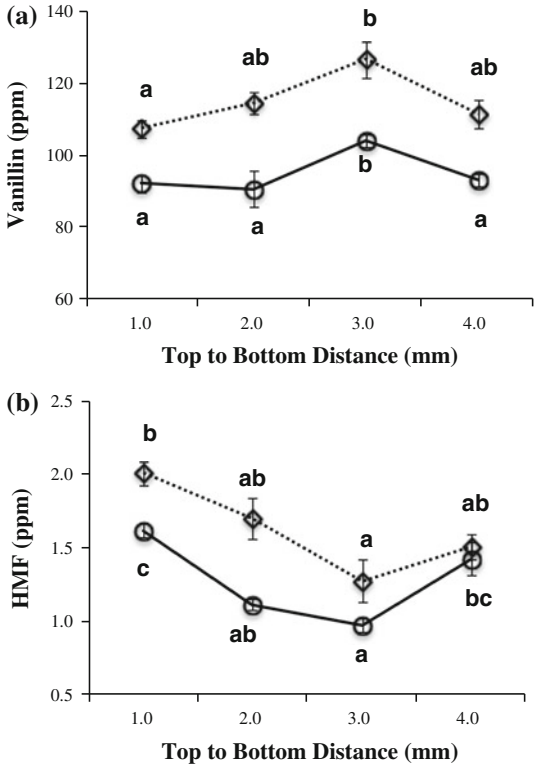

Fig. 7 Average concentration (ppm) of **a** vanillin and **b** HMF calculated for four layers cutting from top to bottom for PG biscuits (*full lines*) and TA biscuits (*dotted lines*) with *error bars* displayed as ±SE. *Different letters* indicated significant different levels between layers ($p < 0.05$)

contained the lowest concentration of vanillin, this is presumably due to radiative heating leading to the thermal damage at the surface and conductive heating at the base, which can be supported the mass transfer modelling predictions of Sakin [22]. As previously detailed, TA biscuits contained reproducibly greater vanillin after baking than PG biscuits, which was consistent across all slices of all biscuits, which may be due to enhanced moisture diffusivity driven by the higher porosity in the PG biscuits [23].

Horizontal distribution of HMF across the biscuit structure

Distribution of HMF concentration (Fig. 8) followed a similar but inverted pattern to vanillin (Fig. 6) when sectioned from left to right (horizontally). The concentration of HMF was the highest at the extremities, apart from the furthest right PG sample which did not show elevated HMF. Orientation was such that the darkest baked side of the biscuit always marked as the left (0 mm) to aid interpretation, which explains the 35-mm PG sample.

The central core of the TA biscuits had the lowest HMF concentration with a maximal 55 % reduction from the left orientation. The largest reduction observed in the PG biscuit was 32 % indicating that a difference in Maillard chemistry occurred between the PG and the TA biscuits or that the components have a higher thermal protection during baking in the TA biscuits. This is comparable to the horizontal vanillin distribution detailed previously.

Vertical distribution of HMF across the biscuit structure

The vertical distribution for HMF (Fig. 7) follows a similar pattern to its horizontal distribution (Fig. 8): the lowest HMF concentration is present in the core of the biscuit, and it can be hypothesised that this region would have received the least heat damage [22]. HMF generation is a bi-product of Maillard chemistry, and its formation is strongly linked to thermal exposure, a good example is the high concentrations found in the crust of bread when compared to the crumb [24].

Figure 9 shows the horizontal distribution of pores and relative porosity by analysed layer, TA biscuits had a central core of the biscuit that contained larger pores and lower porosity than that of the PG biscuits which correlates with the higher retention of vanillin in the central core of the TA biscuit shown previously (Fig. 7). Diffusivity is strongly correlated to porosity in bread systems, and although there are a large number of interacting variables, Baik [23] has shown that matrices with the highest porosity during baking can have the highest moisture diffusivity,

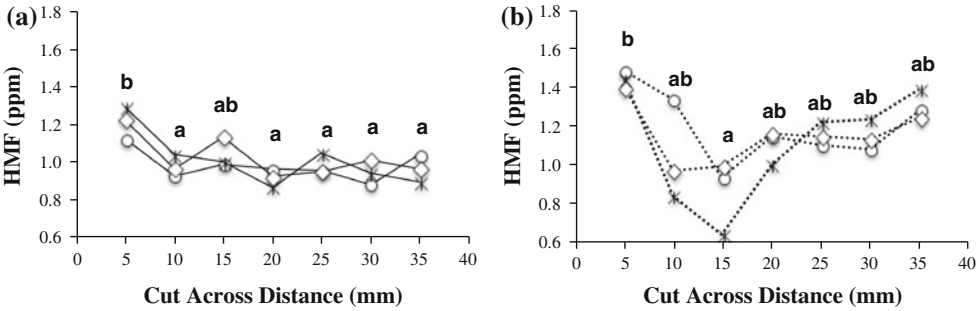

Fig. 8 Distribution of HMF concentration (ppm) cutting across seven pieces for **a** three PG biscuits (*full lines*) and **b** three TA biscuits (*dotted lines*). *Different letters* indicated significant different levels between pieces ($p < 0.05$)

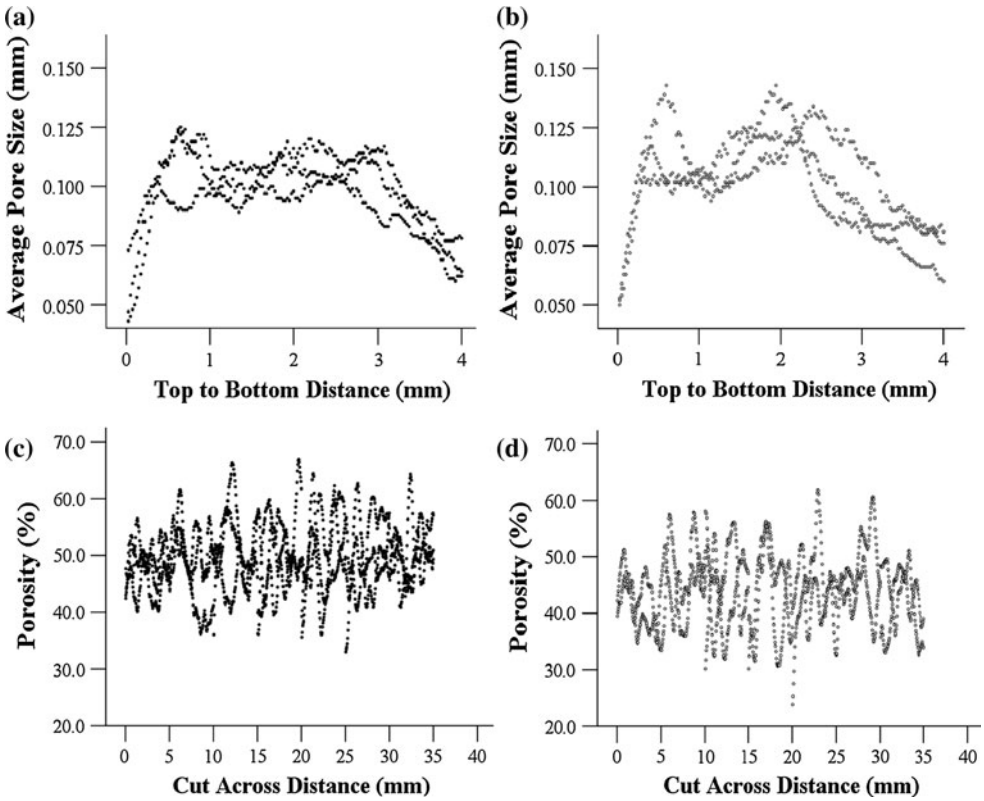

Fig. 9 Scatter plot of average pore size (mm) cutting from top to bottom of **a** three PG biscuits (*black dots*) and **b** three TA biscuits (*grey dots*). Scatter plot of average porosity (%) cutting across from left to right of **c** three PG biscuits (*black dots*) and **d** three TA biscuits (*grey dots*)

this could lead one to propose that the higher porosity of the PG sample would be linked to higher moisture loss, greater thermal damage in the core of the biscuit and higher loss of vanillin through volatilisation, which may explain the enhanced stability of vanillin in TA biscuits when compared to PG biscuits.

Previous studies [25] have also applied a quantitative study on biscuit micro-structure from different sections, and their results showed that protein, fat and total starch are evenly distributed throughout the structure of the biscuit. They also found greater gelatinised starch in the middle regions compared with upper and lower surfaces and explained that during baking heat penetrates from the upper and lower surfaces that these surfaces heat up faster than the central core and that aerating agents (carbon dioxide and ammonia) are therefore lost more quickly in the hotter regions. The aerating agents (plus the production of steam) in the central region have more time to act which is proposed to be linked to a higher number of pores being produced. Similarly, moisture is removed very quickly from the surface, but the rate of moisture loss is slower in the core of the biscuit, allowing greater concentrations of gelatinised starch to be generated. Since aroma compounds can reversibly interact with starch [26], vanillin may also receive a chemical thermal protection in the central core.

Conclusion

In conclusion, it was shown that vanillin concentration was highest in the centre of biscuits, and HMF concentration was highest at the surface of the biscuit, and that in general, PG biscuits had greater porosity but smaller pore diameter when compared to TA biscuits. In addition, there was a significant effect of solvent type (TA, PG) on the distribution of vanillin and HMF across the biscuit matrix with biscuits made with TA as the flavour solvent having the greatest concentration of HMF and vanillin.

This study illustrates how X-ray μCT can be employed as a valuable tool to non-destructively visualise the internal biscuit structure and provide quantitative information on the internal pore structure and, in conjunction with aroma distribution analysis, can help to explain how choice of flavour solvent may impact biscuit micro-structure and the generation and stability of aroma compounds.

Acknowledgments This work was supported by a Knowledge Transfer Partnership awarded to Aromco Ltd. and the University of Nottingham by Technology Strategy Board, UK. The help of Professor Andy Taylor, Paul Yeomans, Jackie Harvey and Ray McKee in setting up this project is acknowledged.

References

1. Acrctander S (1969) Perfume and flavor chemicals, 6th edn. Steffen Arctander's Publications, Las Vegas
2. Bartlett GR (1959) Phosphorus assay in column chromatography. J Biol Chem 234:466–468
3. Heydanek MG, Min DBS (1976) Carbonyl-propylene glycol interactions in flavor systems. J Food Sci 41:145–147
4. Potineni RV, Peterson DG (2008) Mechanisms of flavor release in chewing gum: Cinnemaldehyde. J Agric Food Chem 56:3260–3267
5. Elmore JS, Dodson AT, Mottram DS (2011) Reactions of propylene glycol with the constituents of food flavourings. In: The thirteenth Weurman Flavour Research Symposium. Book of Abstracts: Zaragoza, Spain, p 137
6. Choi SJ, Decker EA, Henson L, Popplewell LM, McClements DJ (2009) Stability of citral in oil-in-water emulsions prepared with medium-chain triacylglycerols and triacetin. J Agric Food Chem 57:11349–11353
7. De Roos KB (2007) Modifying flavour in food. In: Taylor AJ, Hort J (eds) Woodhead Publishing Ltd., Cambridge, pp 243–273
8. Potineni R, Peterson D (2008) Influence of flavor solvent on flavor release and perception in sugar-free chewing gum. J Agric Food Chem 56:3254–3259
9. Babin P, Della Valle G, Dendievel R, Lourdin D, Salvo L (2007) X-ray tomography study of the cellular structure of extruded starches and its relations with expansion phenomenon and foam mechanical properties. Carbohydr Polym 68:329–340
10. Kerckhofs G, Schrooten J, Van Cleynenbreugel T, Lomov SV, Wevers M (2008) Validation of X-ray microfocus computed tomography as an imaging tool for porous structures. Rev Sci Instrum 79:13711
11. Feldkamp LA, Davis LC, Kress JW (1984) Practical cone-beam algorithm. J Opt Soc Am A-Opt Image Sci Vis 1:612–619
12. Frisullo P, Conte A, Del Nobile MA (2010) A novel approach to study biscuits and breadsticks using X-ray computed tomography. J Food Sci 75:E353–E358
13. Ledl F, Severin T (1978) Browning reactions of pentoses with amines.13. Investigation of the Maillard reaction. Z Lebensm-Unters-Forsch 167:410–413
14. Fisk ID, Linforth RST, Taylor AJ, Gray DA (2011) Aroma encapsulation and aroma delivery by oil body suspensions derived from sunflower seeds (*helianthus annus*). Eur Food Res Technol 232:905–910
15. Abramoff MD, Magalhaes PJ, Ram SJ (2004) Image processing with image. J Biophoton Int 11:36–42
16. Chevallier S, Colonna P, Buleon A, Della Valle G (2000) Physicochemical behaviors of sugars, lipids, and gluten in short dough and biscuit. J Agric Food Chem 48:1322–1326
17. Chevallier S, Colonna P, Lourdin D (2000) Contribution of major ingredients during baking of biscuit dough systems. J Cereal Sci 31:241–252
18. Lara E, Cortes P, Briones V, Perez M (2011) Structural and physical modifications of corn biscuits during baking process. LWT- Food Sci Technol 44:622–630
19. Sakin M, Kaymak-Ertekin F, Ilicali C (2007) Simultaneous heat and mass transfer simulation applied to convective oven cup cake baking. J Food Eng 83:463–474
20. Kayaci F, Uyar T (2012) Encapsulation of vanillin/cyclodextrin inclusion complex in electrospun polyvinyl alcohol (pva) nanowebs: prolonged shelf-life and high temperature stability of vanillin. Food Chem 133:641–649
21. Yang N, Hort J, Linforth R, Taylor A, Brown K, Walsh S, Fisk ID (2011) Aroma and flavour solvent: impact on the matrix. XIII Weurman Flavour Research Symposium, Zaragoza
22. Sakin-Yilmazer M, Kaymak-Ertekin F, Ilicali C (2012) Modeling of simultaneous heat and mass transfer during convective oven ring cake baking. J Food Eng 111:289–298
23. Baik O-D, Marcotte M (2003) Modeling the moisture diffusivity in a baking cake. J Food Eng 56:27–36
24. Ramirez-Jimenez A, Guerra-Hernandez E, Garcia-Villanova B (2000) Browning indicators in bread. J Agric Food Chem 48:4176–4181
25. Burt DJ, Fearn T (1983) A quantitative study of biscuit microstructure. Starch Stärke 35:351–354
26. Kant A, Linforth RST, Taylor AJ (2003) Flavour retention and release from starch solutions Flavour research at the dawn of the twenty-first century. Éditions Tec & Doc, Dijon, pp 103–106